MATEC Web of Conferences **14**, 13007 (2014)
DOI: 10.1051/matecconf/20141413007

Removal of casting defects from CMSX-4® and CMSX-10® alloys by electropolishing in a novel electrolyte; Deep Eutectic Solvent

Neil Dsouza[1], Matthew Appleton[2], Andrew Ballantyne[3], Amy Cook[3], Robert Harris[3], and Karl S. Ryder[3]

[1] Rolls-Royce plc, Elton Road, PO. Box 31, Derby DE24 8BJ, UK
[2] Department of Materials Science and Metallurgy, University of Cambridge, 27 Charles Babbage Road, Cambridge CB3 0FS, UK
[3] Department of Chemistry, University of Leicester, University Road, Leicester LE1 7RH, UK

Abstract. Here we describe the use of environmentally benign Deep Eutectic Solvents (DESs) to electropolish oxide casting scale from Ni based superalloy turbine blades. These new electrolytes are a viable alternative to hazardous and aggressive aqueous acids and etchants currently used to process these components. In addition we show that the DES electrolytes selectively expose the underlying surface structure of these superalloys. We demonstrate the ability of these electrolytes to preferentially etch either γ or γ' phases depending on the choice of electrolyte formulation and the applied potential during the electrolytic etch on CMSX-4® and CMSX-10® alloys.

Introduction

Single crystal superalloy casting methodologies are now common place for the manufacture of turbine components of aerospace engines where the components are subjected to extreme thermal and mechanical stresses. Typically, such components, for example turbine blades, can be expected to operate at temperatures 200–300 °C above the melting point of the alloy and so demands in performance are great. Typical single crystal superalloys castings are manufactured using the vacuum investment casting process; during this process the molten superalloy is poured in a ceramic mould that has been fabricated *via* the lost wax method [1–5]. The single crystal growth is controlled in part by the speed and temperature at which this mould is removed from the furnace. Once solidified the structure of the single crystal is based around a dendritic core surrounded by eutectic regions of the superalloy. Further heat treatment is required to homogenise the superalloy so that all regions of the single crystal exhibit the same performance capabilities. This homogenised structure consists of two distinct regions, a thin lattice-structured γ phase and a cubic-structured γ' phase. The γ' phase occupies approximately 70% of the overall volume and elements in the superalloy such as Al, Ti, Ta are found in the highest concentrations in this region. Elements such as, Cr, Re, W, tend to aggregate towards and remain in the γ phase [6–12]. During withdrawal from the furnace and subsequent solidification, surface oxide scale is often formed on the casting as a result of the differential thermal contraction of the ceramic mould and the cooling metal. The differential cooling rates can result in regions of exposed superalloy which can oxidise to form mixed metal oxide species, also known as casting scale, at the surface. Formation of scale on aerofoil turbine blades poses a significant issue for critical inspection of potential recrystallization (RX) grains. The presences of RX grains can cause critical failure during operation, and so inspection of the turbine blades for RX is important. In addition to obscuring grain structure inspection, residual casting scale is also associated with instances of surface incipient melting during heat treatment. This can result in the formation of melt pools and new RX grains in the surface of the casting. Mechanical removal of the surface scale prior to heat treatment can also induce the formation of new RX grains and so the most commonly used method to remove this surface scale is *via* electrolytic etching [6]. Conventionally the electrolytes used for this process are highly hazardous and corrosive, for example mixtures of nitric/phosphoric and sulphuric acid, which can be difficult and unpleasant to handle, are environmentally damaging and can also cause unwanted pitting and uneven etch rates of the surface of the casting during the electrolytic etch [13].

Previously we have described a novel alternative to these types of electrolytes by using Deep Eutectic Solvents (DESs) to successfully remove the surface scale [12]. DESs are low toxicity ionic solvents based around complexing a quaternary ammonium salt (QAS) with a hydrogen bond donor (HBD) (alcohols/amines/carboxylic acids etc.) [14, 15]. The role of the HBD in these mixtures is to complex to the halide anion of the QAS, which in turn will cause a decrease in the lattice energy of the of the high melting QAS, resulting in a system that is often fluid at room temperature. They can be described by the general formula;

$$R_1R_2R_3R_4N^+[X^- \cdot zY]. \quad (1)$$

Where $R_1R_2R_3R_4N^+$ describes the QA component of the DES, X^- the halide anion bound to the QA cation and z Y which describes the HBD and number of equivalents. The mixtures resulting from complexing a QAS with one of a number of HDB's, are low melting ionic solvents that generally have a wide electrochemical window, good conductivity and a high affinity for metal salts which makes them good candidates for electropolishing/etching of most metal surfaces. They have been shown to be suitable alternatives to current electropolishing electrolytes for stainless steels as well as other high value/performance alloys and have been employed in full industrial scale up applications [14–17].

In our previous work we have demonstrated that electropolishing in DES electrolytes can be effective in removing oxide scale from as cast components prior to heat treatment. This methodology subsequently enables grain inspection and the identification of faulty castings prior to heat treatment and also prevents the formation of incipient melting during heat treatment [12]. Here we describe an extension of these studies and will focus on a discussion of the effect of electrolyte formulations and applied potential on the surface morphology of two superalloys CMSX-4 and CMSX-10 during electropolishing in DESs.

Experimental details

Described below are the methodologies and materials for the formation of all DESs used for the electropolishing of CMSX-4 and CMSX-10. The DES we use here are, for brevity, referred to by their trade name as described by the bulk manufacturing company, Scionix Ltd.

Preparation of DES

Ethaline 200

Choline chloride [$HOC_2H_4N(CH_3)_3Cl$] (ChCl) (Aldrich 99%) was recrystallized from absolute ethanol, filtered and dried under vacuum. Ethylene glycol (EG) (Aldrich 99%), was used as received. The eutectic mixtures were formed by stirring the two components together, in a stoichiometric ratio 2EG:1ChCl, at 70 °C until a homogeneous, colourless liquid formed.

Glyceline 200

Choline chloride [$HOC_2H_4N(CH_3)_3Cl$] (ChCl) (Aldrich 99%) was recrystallized from absolute ethanol, filtered and dried under vacuum. Glycerol (Gly) (Aldrich 99%), was used as received. The eutectic mixtures were formed by stirring the two components together, in a stoichiometric ratio 2Gly:1ChCl, at 70 °C until a homogeneous, colourless liquid formed.

Oxaline 100

Choline chloride [$HOC_2H_4N(CH_3)_3Cl$] (ChCl) (Aldrich 99%) was recrystallized from absolute ethanol, filtered and dried under vacuum. Oxalic acid dihydrate (OXDH) (Aldrich 99%), was used as received. The eutectic mixtures were formed by stirring the two components together, in a stoichiometric ratio 1OXDH:1ChCl, at 50 °C until a homogeneous, colourless liquid formed.

Reline 200

Choline chloride [$HOC_2H_4N(CH_3)_3Cl$] (ChCl) (Aldrich 99%) was recrystallized from absolute ethanol, filtered and dried under vacuum. Urea (Ur) (Aldrich 99%), was used as received. The eutectic mixtures were formed by stirring the two components together, in a stoichiometric ratio 2Ur:1ChCl, at 50 °C until a homogeneous, colourless liquid formed.

Acetaline 200

Choline chloride [$HOC_2H_4N(CH_3)_3Cl$] (ChCl) (Aldrich 99%) was recrystallized from absolute ethanol, filtered and dried under vacuum. Glacial acetic acid (ACA) (Aldrich 99%), was used as received. The eutectic mixtures were formed by stirring the two components together, in a stoichiometric ratio 2ACA:1ChCl, at 70 °C until a homogeneous, colourless liquid formed.

Experimental setup

Heat treated test bars of CMSX-4 and CMSX-10 were received from Rolls-Royce, sectioned and mounted in Bakelite resin, in which the exposed surfaces were mechanically polished to a mirror finish using various roughness grades of polishing cloths from 9 μm down to 0.25 μm. Electrical contacts were made by drilling and tapping holes in the reverse side of the mount and then inserting a stainless steel screw to achieve contact. The resin block with an "O ring" embedded in the outer surface was then inserted into the bottom of a bespoke glass cylinder. Approximately 30 mL of DES at a temperature of 40 °C was then placed into the cell. The cathode used for these experiments was constructed from a Ti mesh coated in IrO. The mesh was 10 cm L × 3 cm W and moulded into an L shape with the lower part being 3 cm in length. The cathode was placed approximately 2 cm above the anode in the electrolyte. To insulate other regions/test bar samples in the resin block and silicone insulating tape was applied to surfaces that were not required to be etched. Dissolution rates during electropolishing were estimated by measuring the resultant step height, using atomic force microscopy (AFM), at the edge between masked (insulated) and unmasked (exposed) areas of the superalloy surfaces after electrolytic etching.

Surface characterisation

Scanning Electron Microscopy (SEM)

A Phillips XL-30 Field Emission Gun scanning electron microscopy (FEG SEM) was used equipped with a Bruker AXS XFlash 4010 EDS detector operating at 25 kV. Secondary electron imaging (SEI) was performed with a working distance of ca. 5 mm and accelerating voltage of ca. 20 kV.

Table 1. Selected elemental composition of CMSX-4 and CMSX-10.

	CMSX-4	CMSX-10
Al	5.58%	5.78%
Co	9.65%	3.3%
Cr	6.4%	2.25%
Re	2.95%	6.3%
Ta	6.53%	8.2%
W	6.4%	5.45%
Ni	~60%	<68%

Atomic Force Microscope (AFM)

AFM images were acquired using a Digital Instruments (DI) Nanoscope IV, Dimension 3100 instrument using resonant (tapping) mode (software version 6.12).

Optical profilometry

3D optical images were captured on a Zeta Instruments Zeta 2000 optical profiler using the inbuilt Zeta3D software version 1.8.5.

Results and Discussion

The removal of casting scale is an important part of the processing of the aerofoil castings, however, the effects on the surface morphology of the underlying metal postelectropolishing, have not previously been discussed. Here we investigate the effects of different DESs based on ChCl. This work also looks at the effect of different potentials applied during the etching process. The surface morphology has been investigated in two separate superalloys CMSX-4 (2nd generation Ni-based superalloy) and CMSX-10 (3rd generation Ni-based superalloy) and comparisons between the different phase selectivities for each superalloy are reported. The etch rates of CMSX-4 as a function of potential and time are also investigated here. Table 1 shows selected elemental compositions of CMSX-4 and CMSX-10.

As shown in Table 1, there are a few important differences in the elemental composition of these two superalloys. Firstly the content of the elements such as Co and Cr, which are used primarily for corrosion resistance, are lower in the 3rd generation CMSX-10. Other elements, such as Re and Ta are found in higher concentration in CMSX-10 than in CMSX-4. The role of these refractory elements is to increase the melting temperature and creep resistance of the superalloy. CMSX-10 also has approximately 20 other metallic elements additional to the ones in CMSX-4, such as Mn, Ag, As, Ga, Pt, Sn, Fe although the concentration of these elements fall below 100 ppm. A comparison of DES physical properties are shown in Table 2.

The rheological properties of the liquid are very sensitive to the composition. These electrolytes can be several orders of magnitude higher in viscosity than the conventional aqueous electrolytes, but this can have benefits for the electropolishing mechanism.

Table 2. Viscosity and conductivity data at room temperature for all DES used to electropolish CMSX-4 and CMSX-10.

DES	Viscosity/ cP	Conductivity/ mS cm^{-1}
Ethaline 200	38	6.58
Glyceline 200	376	1.05
Oxaline 100	286	2.54
Reline 200	721	0.55
Maline 100	1070	0.35
Acetaline 200	64	4.29

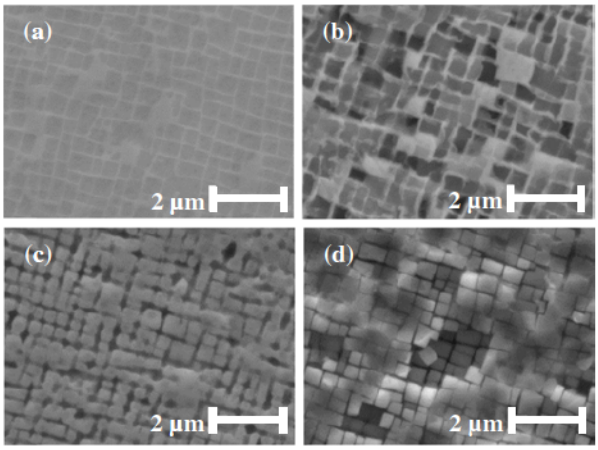

Figure 1. SEM images of surface morphology of CMSX-4 pre and post-electropolish using Ethaline 200. (a) No applied potential, (b) 2 V, (c) 4 V, and (d) 5 V.

CMSX-4 and CMSX-10 phase selectivities from electrolytic etching in ethaline 200

Figure 1 shows scanning electron microscope (SEM) images of CMSX-4 pre and postelectropolishing using Ethaline 200. These and all subsequent electropolishing experiments are carried out for a total of 30 minutes unless specified.

In Fig. 1 it can be seen that in the case of CMSX-4, there is a clear change in preference for γ and γ' by changing the potential applied during the electropolishing process. At 2 V (b), there is a preference for attack at the γ' cubes, whilst the γ channels remain intact. By increasing the potential to 4 V there is a switch in the phase selectivity from the γ' cubes to the γ channels. There is some slight dissolution of the edges of the γ' cubes showing that at this potential it is not completely phase selective. By increasing the potential to 5 V the γ channels remain completely etched from the structure, however there is a clear reduction in the dissolution rate of the γ' cubes. This is somewhat surprising since it would be expected that a reduction in the phase selectivity/sensitivity at higher potentials would occur since the oxidation potential for each phase is likely to be far below the applied potential. The images in Fig. 2 shows the surface morphology of CMSX-10 post-electropolishing in Ethaline 200 at potentials of 2, 4 and 8 V (b,c and d) as well as the mechanically polished surface (a).

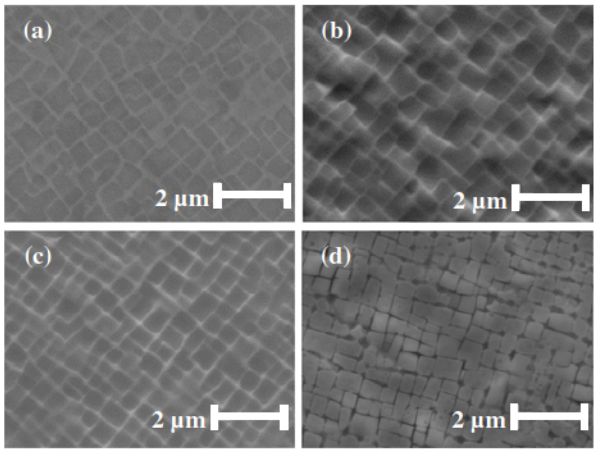

Figure 2. SEM images of surface morphology of CMSX-10 pre and post-electropolish using Ethaline 200. (a) No applied potential, (b) 2 V, (c) 4 V, and (d) 8 V.

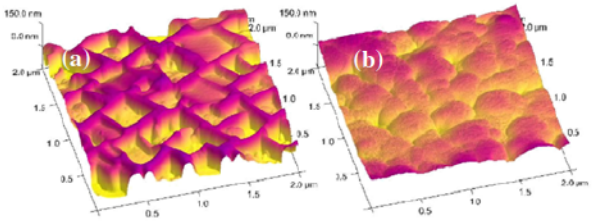

Figure 3. AFM images of CMSX-4 electropolished in Ethaline 200; (a) at 3 V showing γ' cubes removed and (b) at 6 V with γ channels preferentially removed.

The images in Fig. 2 shows a lower sensitivity to potential with respect to phase selectivity using Ethaline 200 as an electrolyte. At both 2 V (b) and 4 V (c) there is a slight etch of the γ' cubes. It isn't until a potential of 8 V is applied that any change in the phase selectivity is observed and the γ channels are selectively etched. Overall it would appear that CMSX-10 is less sensitive to applied potential during etching in Ethaline 200.

AFM has also been used in conjunction with SEM in order to provide topographical information in respect of the electrochcemical processed surfaces, Figs. 1 and 2.

AFM images of CMSX-4 electropolished at 3 V and 6V are shown in Fig. 3. These images clearly show the topographical contrast produced by the selective etching of the respective phases and are consistent with the images presented in Fig. 1.

Etch rate of CMSX-4 in Ethaline 200

An understanding of how much material is removed during the electropolishing of the casting scale is essential for good process control and dimensional conformity. Here we have used AFM to estimate the dissolution rates of CMSX-4 at a number of regular time intervals and applied potentials. This was achieved by masking a small area of the metal during polishing. After polishing, the mask was removed and the step height between the polished and unpolished (masked) areas was measured. The dissolution rates of CMSX-4 at potentials of 2, 3 and 4 V were measured at regular intervals of 5 minutes up to a total of

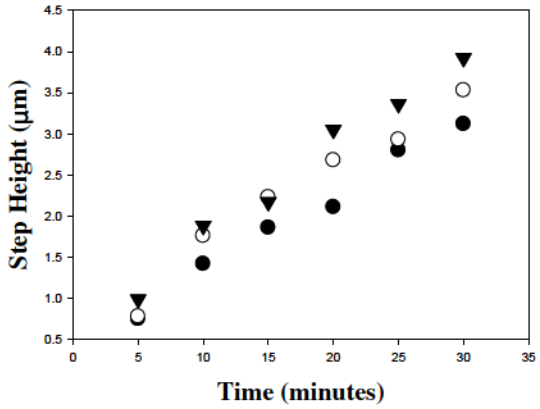

Figure 4. Step height measurements between electropolished and and non-electropolished regions of CMSX-4. Solid circle 2 V, hollow circle 3V, triangle 4 V.

Table 3. Step height measurements between electropolished and and non-electropolished regions of CMSX-4, Fig. 4.

	Step Height/μm		
Time (mins)	**2 V**	**3 V**	**4 V**
5	0.75	0.78	0.99
10	1.42	1.76	1.88
15	1.86	2.23	2.17
20	2.11	2.68	3.05
25	2.80	2.93	3.36
30	3.12	3.53	3.92

30 minutes. Graphical representation of the step heights measured can be seen in Fig. 4 and the raw data are presented in Table 3.

The data in Fig. 4 show a linear etch rate for all applied potentials. Increasing the magnitude of the applied potential has the anticipated effect of increasing measured current and dissolution rate of the superalloy.

Measurement of the dissolution rates by AFM in this way is limited by the maximum extent of transverse $(x - y)$ motion of the scanning head (here $100 \times 100\,\mu$m) and by the maximum distance of travel in the z-direction, perpendicular to the plane of the metal surface (here $8\,\mu$m). These physical constrains consequently limit the time and distance scales over which dissolution changes can be measured. In order to measure these dissolution rates over much larger distances and longer times we have very recently used focus variation microscopy using the Zeta Instruments Zeta 200 3D optical profiler. Here a 3D topographical image can be obtained over areas of several mm^2 and height ranges of mm. A typical 3D image and profile plot of the step can be seen in Fig. 5.

The image presented as Fig. 5a shows a 3D representation of the area between the electropolished and non-electropolished regions of the CMSX-4. The data shown in Fig. 5b represent a line trace across the step defining the boundary between the unpolished (*left*) and polished (*right*) regions. Interestingly these data show a marked under-cut close the boundary between the masked and unmasked regions and this is a typical artefact of electrochemical etching at a mask. This suggests that a more accurate determination of dissolution rate would

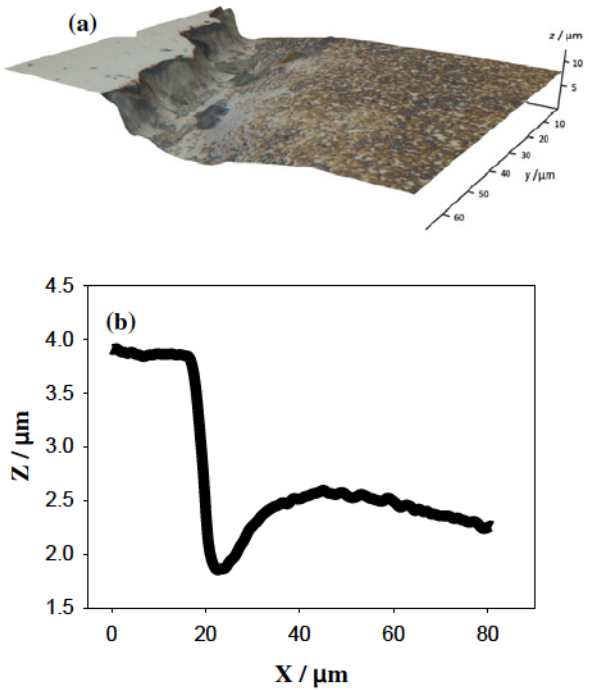

Figure 5. 3D image (a) of the step between non-electropolished and electropolished regions (footprint region 80 μm x 70 μm) and (b) profile data of the step between non-electropolished and electropolished regions of CMSX-4 at 4 V after 30 minutes in Ethaline 200.

be obtained by integrating the volume of removed metal (below the plane defined by the un-etched region) using the data obtained from the 3D image. An evaluation of this approach is part of our on-going studies.

CMSX-4 and CMSX-10 phase selectivity behaviour using alternative DES

Alternative DESs to Ethaline 200, have been investigated, including Oxaline 100, Reline 200, Glyceline 200, Maline 100 and Acetaline 200 to determine whether the electrolyte plays as key a role in the selective dissolution of γ and γ' phases and whether it can be chosen selectively to yield a specific phase selectivity. These DESs were chosen based on their physical properties and the acidic/basic nature of the HBD. Both CMSX-4 and CMSX-10 were electropolished using these alternative electrolytes. The applied potentials of the electropolishing are 2, 3, 4, 5 and 8 V however only 2 and 5 V will be shown for comparison between the two superalloys.

Oxaline 100

Oxaline 100. a DES formed by combining a oxalic acid dihydrate with ChCl, was used to electropolish both CMSX-4 and CMSX-10. The surface morphology at applied potentials of 2 V (left column) and 5 V (right column) can be seen in Fig. 6.

Figure 6 shows the morphology of the etched surface of both CMSX-4 and CMSX-10 at selected potentials of 2 V and 5 V. Unlike the phase selectivities seen for

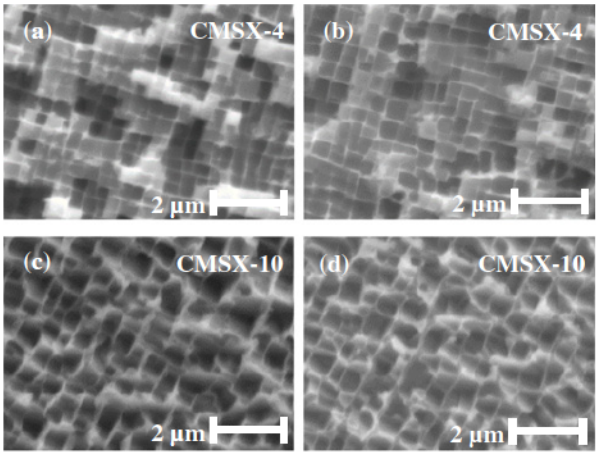

Figure 6. SEM images of CMSX-4/10 post- electropolish using Oxaline 100 at 2 V (a, c) and 5 V (b, d).

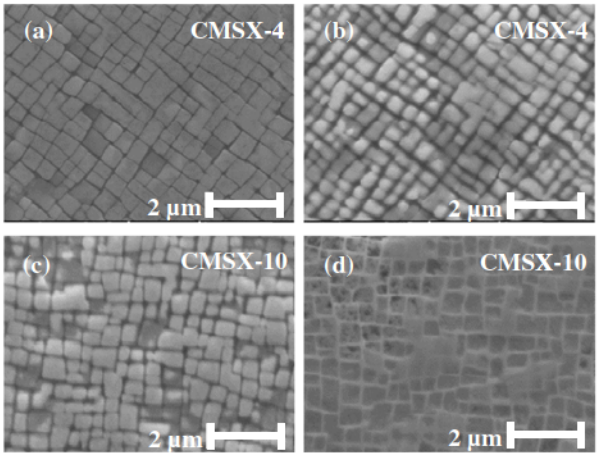

Figure 7. SEM images of CMSX-4/10 post-electropolish using Reline 200 at 2 V (a, c) and 5 V (b, d).

Ethaline 200 in both superalloys (Fig. 1 and Fig. 2), there is no change in which phase is preferentially etched when different potentials are applied. Clearly there is a preference for γ' cube dissolution and very little in the way of apparent attack of the γ channels. The fact that there is no switch in phase selectivity could indicate an interesting property of the electrolyte. The water of hydration on the oxalic acid could be effectively acting as a sacrificial additive at higher potentials increasing the overall activity of the oxalic acid. The effect is more pronounced in the CMSX-10 samples rather than the CMSX-4. The higher levels of refractory elements found in the γ channels could be a key influence in the phase selectivity in this electrolyte since these oxides are likely to be less soluble and are also more likely to passivate the surface.

Reline 200

Reline, a DES formed by combining a urea with ChCl, was subsequently used to electropolish both CMSX-4 and CMSX-10. The surface morphology at applied potentials of 2 V (left column) and 5 V (right column) can be seen in Fig. 7.

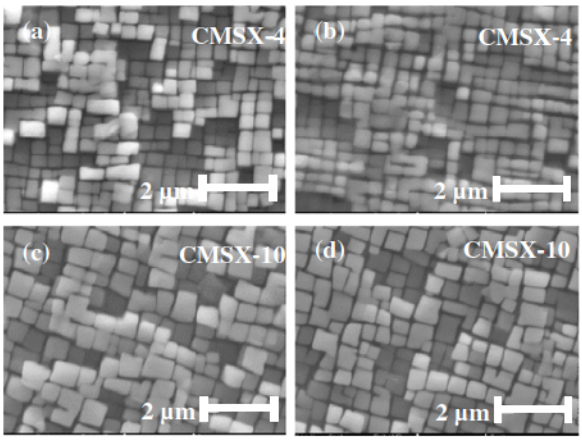

Figure 8. SEM images of CMSX-4/10 post-electropolish using Glyceline 200 at 2 V (a, c) and 5 V (b, d).

Figure 7 shows that the phase selectivity of Reline 200 is primarily effected on the γ channels, this is in contrast to the phase selectivities observed using Oxaline 100 (Fig. 6). In CMSX-4 at low potentials (2 V) there is a clear focus on dissolution of the γ channels with little to no etching of the γ' cubes. At higher potentials (5 V) the selectivity is still focused on the γ channels however the γ' cubes are no longer smooth with straight edges. The edges of the γ' cubes are becoming rounded suggesting that attack is slowly taking place around the edges of these cubes once the γ channels have been removed. In CMSX-10 at 2 V the γ channels are removed with some slight etching of the γ' cubes around the edges. At 5 V however there is a switch in the phase selectivity where the γ' cubes become the preferred phase for dissolution. This in particular is in contrast to the phase selectivity observed for CMSX-4 at the same potential.

Glyceline 200

The images in Fig. 8 show surface morphology using a DES formed by combining glycerol with ChCl.

The images in Fig. 8 shows SEM images post electropolishing of the two superalloys using Glyceline 200 as the electrolyte. There is clear preference for the γ channels at all potentials applied. The images show regions where γ' cubes have been lost from the surface which would suggest that the γ channels are also being etched underneath these cubes allowing them to fall from the surface of the superalloy. Such selectivity for the γ channels may not necessarily be expected, especially when compared to the results seen for Ethaline 200 in Figs. 1 and 2. The addition of a central CHOH group to ethylene glycol to form glycerol, increasing the number of OH groups from 2 to 3, may not drastically change the electrolyte chemically, but the change in physical properties may play a key factor during the etch rates. Typically at room temperature Glyceline 200 will have a viscosity approximately an order of magnitude higher than Ethaline 200 and the conductivity almost an order magnitude lower.

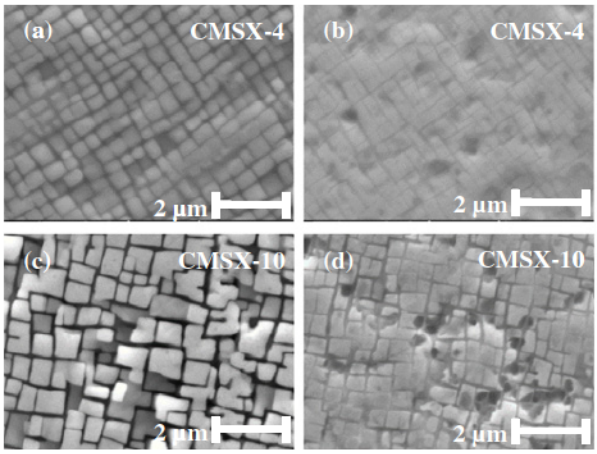

Figure 9. SEM images of CMSX-4/10 post-electropolish using Maline 100 at 2 V (a, c) and 5 V (b, d).

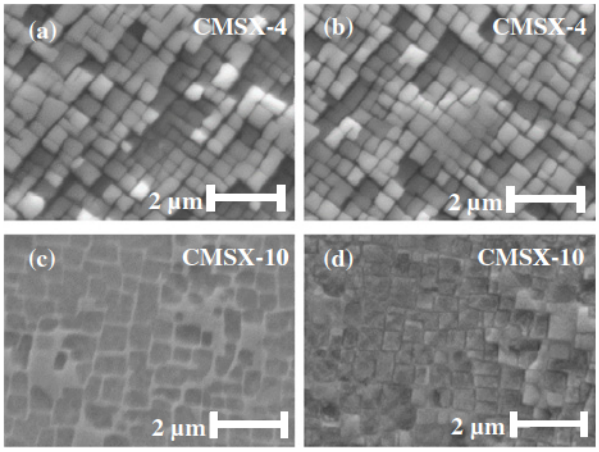

Figure 10. SEM images of CMSX-4/10 post-etch using Acetaline 200 at 2 V (a, c) and 5 V (b, d).

Maline 100

The images in Fig. 9 show surface morphology using a DES formed by combining malonic acid with ChCl.

At low potentials (2 V) the selectivity is almost completely selective to the γ channels in both superalloys, however at higher potentials (5 V) the electrolyte appears to lose its ability to selectively etch either phase and begins to cause pitting, primarily at the three phase boundary regions between γ and γ' phases. The chemical structure of Maline 100 is similar to Oxaline 100 except there is an additional, relatively chemical, inert CH_2 group in the centre of the oxalic acid molecule chain. This HBD also does not contain the two waters of hydration as is the case with Oxaline 100. The chemical variations between Oxaline 100 and Maline 100 are relatively subtle and yet the effect on the electropolish characteristics are very notable.

Acetaline 200

The images in Fig. 10 show surface morphology using a DES formed by combining glacial acetic with ChCl.

Figure 10 shows the etching effects on the surface of both CMSX-4 and CMSX-10 at both 2 V and 5 V.

Clearly, for CMSX-4, the effect is similar to that seen in Glyceline 200 (Fig. 8), where the γ channels are selectively etched and the γ' cubes are unaffected. In CMSX-10, at low potentials there appears to be very little in the way of etching. The surface morphology for CMSX-10 at 2 V closely resembles that of the mechanically polished regions shown in the Ethaline 200 experiments (Fig. 2a). At higher potentials some etching of the γ channels occurs but at much slower rate than that seen in CMSX-4. This is perhaps the most surprising result of all the DES used as it has relatively high conductivity, low viscosity and the starting HBD is the most acidic and aggressive of the HBD's yet arguably performs the worst in terms of being able to expose the underlying surface morphology.

Conclusions

Here we show that electrochemical polishing of CMSX-4 and CMSX-10 using a range of DES electrolytes results in selectivity of dissolution for the γ and γ' phases, moreover we show that selectivity is a function of the formulation of the electrolyte as well as the applied potential and that the two alloys respond differently to other electropolishing candidates. The DES Ethaline 200 exhibited the most sensitivity to applied potential for CMSX-4 where a clear switch in phase selectivity was observed. At low potentials the preference was for the γ' cubes but at higher potentials the preference switched to the γ channels. For CMSX-10 there was no preference for the γ channels until larger potentials were applied (8 V). Oxaline 100 showed complete selectivity for the γ' cubes at all potentials in both superalloys. In Reline 200 CMSX-4 was only etched in the γ channels at all applied potentials however there was a switch in phase selectivity for CMSX10 where γ was removed at 2 V and γ' at 5 V. In Glyceline 200, there was complete selectivity for the γ channels at all applied potentials. Maline 100 also showed preference for γ channels at low potentials however pitting occurred in the surface at higher potentials (5 V) for both superalloys. For CMSX-4 Acetaline 200 selectively etched the γ channels at all potentials, where as in CMSX-10 any electropolishing was minimal even at 5 V.

The authors are gratefully indebted to the TSB for funding (19088-138212). KSR also wishes to thank the Royal Society for funding under the Industry Fellowship Scheme (IF090090), Rolls-Royce plc for the provision of test material and Zeta Instruments for collaborative development work and helpful discussions regarding sample analysis using 3D optical profiling.

References

[1] G. Brewster, H. B. Dong, N. R. Green and N. D'Souza, Metall. Mater. Trans. B-Proc. Metall. Mater. Proc. Sci., 2008, **39**, 87-93
[2] H. J. Dai, H. B. Dong, N. D'Souza, J. C. Gebelin and R. C. Reed, Metall. Mater. Trans. A-Phys. Metall. Mater. Sci., 2011, **42A**, 3439-3446
[3] H. J. Dai, N. D'Souza and H. B. Dong, Metall. Mater. Trans. A-Phys. Metall. Mater. Sci., 2011, **42A**, 3430–3438
[4] N. D'Souza, R. Beanland, C. Hayward and H. B. Dong, Acta Mater., 2011, **59**, 1003–1013
[5] H. T. Pang, H. B. Dong, R. Beanland, H. J. Stone, C. M. F. Rae, P. A. Midgley, G. Brewster and N. D'Souza, Metall. Mater. Trans. A-Phys. Metall. Mater. Sci., 2009, **40A**, 1660–1669
[6] R. C. Reed, The Superalloys: Fundamentals and Applications, Cambridge University Press, 2006
[7] A. Heckl, R. Rettig and R. F. Singer, Metall. Mater. Trans. A-Phys. Metall. Mater. Sci., 2010, **41A**, 202–211
[8] A. J. Heidloff, J. Van Sluytman, T. M. Pollock and B. Gleeson, Metall. Mater. Trans. A-Phys. Metall. Mater. Sci., 2009, **40A**, 1529–1540
[9] J. Valdes, S. L. Shang, Z. K. Liu, P. King and X. B. Liu, Metall. Mater. Trans. A-Phys. Metall. Mater. Sci., 2010, **41A**, 487–498
[10] J. S. Van Sluytman, A. La Fontaine, J. M. Cairney and T. M. Pollock, Acta Mater., 2010, **58**, 1952–1962
[11] B. C. Wilson and G. E. Fuchs, Metall. Mater. Trans. A-Phys. Metall. Mater. Sci., 2010, **41A**, 1235–1245
[12] A. P. Abbott, N. Dsouza, P. Withey and K. S. Ryder, Trans. Inst. Metal Finish., 2012, **90**, 9–14
[13] D. Landolt, Electrochim. Acta, 1987, **32**, 1–11
[14] A. P. Abbott and K. J. McKenzie, PCCP, 2006, **8**, 4265–4279
[15] A. P. Abbott, K. S. Ryder and U. Konig, Trans. Inst. Metal Finish., 2008, **86**, 196–204
[16] A. P. Abbott, G. Capper, K. J. McKenzie, A. Glidle and K. S. Ryder, PCCP, 2006, **8**, 4214–4221
[17] E. L. Smith, C. Fullarton, R. C. Harris, S. Saleem, A. P. Abbott and K. S. Ryder, Trans. Inst. Metal Finish., 2010, **88**, 285–291